THERMAL STUDIES ON HEAT SINKS EXPOSED TO SOLAR IRRADIATION

by

Dhanushkodi GANESAN[a*], Venkata Ramanan MADHAVAN[b], and Velraj RAMALINGAM[b]

[a] Society for Applied Microwave Electronics Engineering and Research, Chennai, India
[b] Department of Mechanical Engineering, Anna University, Chennai, India

Original scientific paper
https://doi.org/10.2298/TSCI230110081G

The effect of solar irradiation on the temperature of an electronic device attached to a heat sink is studied. Heat sinks with different surface treatments are considered for this study. The contribution of absorbed solar heat by the Al_2O_3 coated fin surface varies from 2.1% to 12.4% of the heat generated by the electronic devices and it reveals that the amount of solar heat absorbed by the black painted heat sink is almost equal to the heat generated by the electronics system. It is also found that the percentage of heat transfer by radiation varies from 6.2% to 11.0% for commercial finish heat sinks and is as high as 58.7% for a black painted heat sink. The combined effect of emissivity and solar absorptivity is studied to optimize the heat sink. For 10 mm fin height, the black painted heat sink illustrates better performance and for 20 mm and 30 mm fin height, the Al coated heat sink exhibits better performance. The temperature of the electronic device increases when the base area of the heat sink is increased beyond 700 cm^2, which is the optimum base area. When the fin height is increased to 20 mm, the optimum base area for the black painted and Al_2O_3 coated heat sink is also increased to 780 cm^2 and 850 cm^2, respectively, thus reducing the device temperature further. The CFD results are validated with the temperature measurement conducted on the heat sink exposed to solar irradiation.

Key words: *thermal management of electronics, natural-convection heat sink, outdoor application, solar heat absorption*

Introduction

Due to advancements in information technology, the usage of communication systems increases rapidly in the automobile, health, education, and banking industries. Applications like 5G communication systems consist of many modules such as high power RF systems, high speed digital boards, beamforming antennas, power supplies, *etc*. in a single enclosure. This increases the heat dissipation per unit volume [1, 2] of the electronics enclosure. The temperature of the electronic devices increases due to the heat generated during their operation, the typical efficiency of devices such as power amplifiers is less than 40% and the remaining power is dissipated as heat. The aging of semiconductor devices depends on many physical phenomena such as hot carrier injection, bias temperature instability, dielectric breakdown, electromigration, *etc*. and temperature is a major cause for aforementioned phenomena. The reliability analysis of electronic devices reveals that the temperature plays a major role in determining the

* Corresponding author, e-mail: dhanush.sameer@nic.in

mean time between failures and follows the logarithmic function of the chip temperature [3]. It is essential to reduce the temperature to increase the gain and to improve the sensitivity of the system.

Heat sink is the most common methodology adopted to dissipate the heat generated by electronic devices and the heat sink is passive and does not drift its performance over a period. The heat generated by the electronic devices is conducted from a smaller area of the heat sink base to a larger area of fins and then transferred to the surrounding ambient air by convection. Conduction resistance offered during the spreading of heat from the smaller area to the larger area is called internal resistance or spreading resistance of the heat sink. Ellison [4] derived an exact solution find out the spreading resistance of rectangular fins attached to the metal plate. He has incorporated the Newtonian effect using the Biot number and derived the correlations to calculate the spreading resistance of the heat sink. Heat sinks are generally fabricated using Al a good conductor of heat that offers very low spreading resistance. The electronic device temperature is further the function of contact resistance or interface resistance between the chip and the heat sink. Maguire *et al.* [5] conducted a comprehensive study and concluded that the interface resistance contributes about 20% to the temperature rise. This can be reduced by using high conductive epoxy or thermal grease between the power amplifier and the heat sink base. The thermal resistance of the currently available epoxy is in the order of 0.3 °C/W per cm^2. Proper selection of interface material, preparation of the contact surfaces and proper application of the thermal grease on the surfaces improve the thermal performance of the heat sink [6].

Kraus *et al.* [7] derived the correlation find out the heat transferred from a vertical plate under natural-convection. The correlation can be used for the entire range of Rayleigh numbers and both laminar and turbulent flow. This correlation can further be used to calculate the heat transfer from inclined surfaces. Lee [8] studied the thermal performance of heat sinks manufactured by various techniques. Stamping and extrusion are widely used manufacturing techniques and the designer can achieve moderate thermal resistance at a lower cost by stamping and extrusion processes. Bar-Cohen *et al.* [9] described the optimization of an array of fins based on the least material philosophy. The authors optimized the fin spacing and other fin parameters based on their thermal performance. Liou *et al.* [10] revisited the natural-convection from the horizontal heat sink and found that for high profile heat sinks the air-flow from the sides of the heat sink is getting disturbed thus lowering the average heat transfer co-efficient.

Radiation heat transfer plays a major role in the thermal management of electronics under natural-convection scenarios. Rao and Venkateshan [11] investigated the interaction of free convection and radiation in a horizontal fin array. The authors independently calculated the convection and radiation heat transfer from the heat sink and concluded that the additive approach is not valid for isoflux surfaces but can be used for isothermal surfaces. Rao *et al.* [12] used conjugate analysis to study the convection and radiation heat transfer from the horizontal fin array. Wang [13] studied the radiation phenomenon in electronic systems and presented simplified guidelines. Yu *et al.* [14] conducted experiments to study the radiation heat transfer from radial heat sinks under natural-convection. It was concluded that the thermal performance of the heat sink can be improved by optimizing the radiation parameters and the mass of the heat sink can be reduced by 20%. Many researchers [15-17] studied the radiation heat transfer from Al alloy used for the cooling of electronic systems such as power amplifiers, LED*, etc.* From the literature survey, it is concluded that the thermal resistance of the heat sink can be reduced by 15% and the case temperature of the electronic devices can be reduced by 10% compared to improving the radiation heat transfer. Due to outdoor mounting practices, the electronics sys-

tems are exposed to solar irradiation. The temperature of the power amplifier system increases drastically due to solar heating. Ganesan and Ramalingam [18] ascertained that the thermal management of outdoor electronics systems should include the effect of solar heat absorbed by the electronics systems since the effectiveness of the heat sink depends on the solar absorptivity of the fin surface. It is understood from the literature that not much work is reported on the contribution of radiation and solar heat absorption on the thermal performance of heat sinks designed for outdoor applications. Surface properties play a major role in radiation heat transfer as well as solar absorption by the fin surfaces. The objective of this work is to study the percentage of heat transfer that occurs through radiation for various surface finishes commonly used in the thermal management of electronics systems and to concurrently study the effect of surface properties on the solar heat absorbed by the heat sink surfaces.

Many researchers have proposed different fin geometry to achieve a high hydrothermal performance of the heat sink with lesser mass per unit volume. In many outdoor applications such as power supplies, commercial communication systems, *etc.*, the conventional Al plate fin heat sink is considered due to lower fabrication cost, easy maintenance, *etc.*, The objective of this work is to study the effect of solar irradiation on the thermal performance of the parallel plate heat sink for outdoor applications. In the present study, the convection and radiation heat transfer rate from the fin surfaces is predicted for various geometric conditions. The base area of the heat sink is varied from 100-900 cm^2. The fin height is varied from 10-30 mm. The emissivity and solar absorptivity values corresponding to different surface treatments commonly used for the thermal management of electronics systems are considered for this study. Temperature measurement is also conducted on the heat sink exposed to solar irradiation validate the simulation results. This study reveals that the radiation heat transfer rate is more than the natural-convection heat transfer rate in certain surface finishes. The solar heat absorbed by the heat sink surfaces is almost equal to the heat generated by the electronic devices and the optimum heat sink size varies for different surface finishes.

Thermal simulation of heat sink

Heat sinks are the most reliable heat transfer technique used to cool electronic devices. The performance of the heat sink depends on many parameters such as fin height, fin thickness, spacing between the fins, *etc.* The radiation heat transfer rate from the fin surfaces depends on emissivity. When the heat sink is exposed to solar irradiation the amount of solar heat absorbed by the heat sink depends on the solar absorptivity of the fin surfaces. The emissivity and the solar absorptivity are the surface properties that depend on the surface treatment process undergone by the heat sink. In addition the fin geometry, variation of the thermal performance due to various surface treatments is also studied here. The thermal analysis is conducted for the cases such as solar rays parallel to the heat sink base and normal to the heat sink base as shown in fig. 1. The amount of solar heat absorbed by the heat sink varies with orientation since the area of the fin exposed to solar irradiation changes. The steady-state

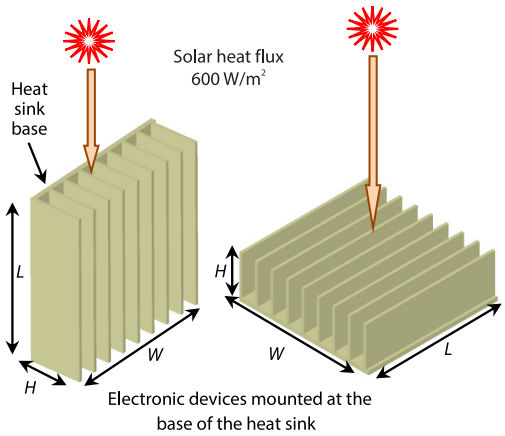

Figure 1. Schematic of orientations of fins exposed to solar irradiation; (a) parallel orientation and (b) normal orientation

heat and fluid-flow analysis are conducted for the heat sink using FloTHERM a commercially available CFD tool. A heat sink with a base area of 200 mm × 300 mm and 3 mm thick is initially considered for the analysis. Since this system is developed for India, the ambient air temperature considered is 40 °C and the corresponding air properties are applied. Rectangular fins of 3 mm thick, 30 mm height, and 300 mm extrusion length are modelled on the heat sink base and the spacing between the fins is maintained as 6 mm.

The Al the commonly used material is considered as the fin material and thermal properties such as thermal conductivity (160 W/mK), specific heat (890 J/kgK), and density (2700 kg/m^3) are given as the input to the CFD tool. It is assumed that the high heat dissipating electronics device such as a power amplifier is mounted on the base of the heat sink and the heat dissipation of 35 W is supplied at the base of the heat sink. The temperature boundary condition is applied for the air volume around the heat sink to represent the constant atmospheric temperature. The heat flux boundary condition is applied on the base of the heat sink to represent the heat generated by the electronic device during its operation. The entire solution domain is divided into finite number of volumes and the following governing equations are applied to each control volume to predict the temperature and flow in each control volume:

– Continuity equation

$$\frac{\partial u}{\partial x}+\frac{\partial v}{\partial y}+\frac{\partial w}{\partial z}=0 \tag{1}$$

– Momentum equation in *X*-direction

$$\rho\left(\frac{\partial u}{\partial t}+u\frac{\partial u}{\partial x}+v\frac{\partial u}{\partial y}+w\frac{\partial u}{\partial z}\right)=\rho g_x-\frac{\partial p}{\partial x}+$$
$$+\frac{\partial}{\partial x}\left[2\mu\frac{\partial u}{\partial x}\right]+\frac{\partial}{\partial y}\left[\mu\left(\frac{\partial u}{\partial y}+\frac{\partial v}{\partial x}\right)\right]+\frac{\partial}{\partial z}\left[\mu\left(\frac{\partial u}{\partial z}+\frac{\partial w}{\partial x}\right)\right] \tag{2}$$

Similarly for *Y*- and *Z*- direction:

– Energy equation

$$\rho C_p\left(\frac{\partial T}{\partial t}+u\frac{\partial T}{\partial x}+v\frac{\partial T}{\partial y}+w\frac{\partial T}{\partial z}\right)=\frac{\partial}{\partial x}\left[k\frac{\partial T}{\partial x}\right]+\frac{\partial}{\partial y}\left[k\frac{\partial T}{\partial y}\right]+\frac{\partial}{\partial z}\left[k\frac{\partial T}{\partial z}\right]+q_v \tag{3}$$

The radiation heat transfer is also concurrently predicted from the fin surfaces. The emissivity value of 0.44 is given as the input to the tool with the assumption that the fin has undergone chrome anodization treatment. The entire solution domain is divided into 2000 grids and the base temperature of the heat sink is predicted. Then the number of grids is gradually increased and the change in base temperature is noted. When the number of grids is increased beyond 2250000 there is no notable change in temperature, thus the grid independent model is developed. Results of the grid independent test are shown in fig. 2. The predicted heat sink base temperature for the parallel orientation is 61.2 °C. The heat sink temperature is predicted for normal orientation also and the predicted base temperature is 62.5 °C. It is further assumed that 600 W/m^2 of solar irradiation is falling on the heat sink [19]. The direction of solar rays is assumed to be parallel to the gravity vector. The solar absorptivity value of $\alpha = 0.56$ is given as the input to represent the chrome anodization surface treatment.

Churchill and Chu [20] proposed a correlation calculate the Nusselt number for vertical and inclined plates subject to natural-convection. The present CFD results are compared with the analytical correlation. Rayleigh number is calculated from the predicted average tem-

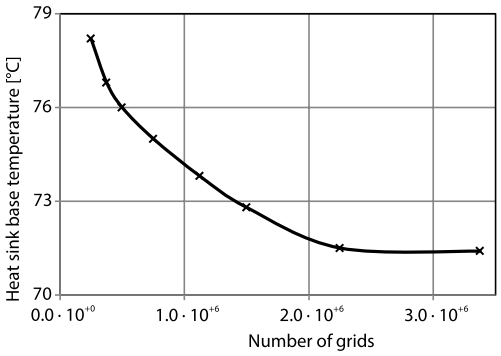

Figure 2. Results of grid independent test

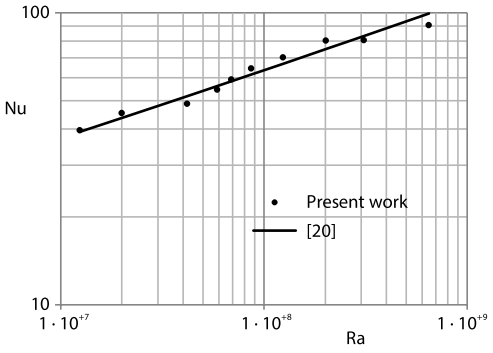

Figure 3. comparison of CFD with analytical results

perature of the fin surface. Nusselt number is calculated from the average heat transfer coefficient predicted by the CFD. The maximum deviation in the CFD results from the analytical correlation is 3.9% and the results are shown in fig 3. The thermal simulation is further repeated with three different surface finishes. The heat sink length and width are varied from 100-300 mm and the fin height is varied from 10 mm to 30 mm. The temperature is predicted for various heat sink base widths, lengths and fin heights. The top edge of the fins receives the solar heat load. Due to solar irradiation falling on the heat sink surfaces, the heat sink base temperature increases marginally by 0.9 °C for the parallel orientation of the heat sink. For normal orientation, the predicted heat sink base temperature is 71.5 °C thus the temperature increases by 9.0 °C due to solar heat absorbed by the heat sink surface. This is due to more surface area being exposed to solar irradiation in normal orientation. This configuration predicts the worst-case temperature scenario of the electronic devices. The temperature distribution on the heat sink is shown in fig. 4. The velocity profile for parallel and normal orientation is shown in fig. 5. The temperature difference along the extruded length of the heat sink fin is 14 °C. The temperature difference between the fin base to tip is 1.8 °C and the temperature variation among the fins is 1.1 °C. The highest temperature is observed at the center of the heat sink base and the same is reported for further discussion.

Experimental validation of CFD results

An experimental set-up is created to conduct the temperature measurement on the heat sink and to validate the computational results. A heat sink with a base area of 200 mm × 300 mm, 30 mm fin height and 6 mm spacing between the fins is fabricated using Al material and chrome anodization surface treatment is done on the heat sink surfaces. A power resistor is used to generate the heat at the base of the heat sink. The power resistor is attached to the base of the heat sink using a fastener. High conductive thermal paste is used between the power resistor and the heat sink base to maximize the contact conductance. The DC power source is used to power up the resistor. The temperature of the power resistor is measured using 24 gauge *T*-type thermocouples. The expanded uncertainty of the thermocouple is ±0.6 °C. The thermocouples are fixed on the base of the heat sink using thermal grease. A Pyranometer made up of a silicon photodiode [21] is used to measure the total solar irradiation falling on the heat sink surfaces. The measurement uncertainty of the Pyranometer is ±3.0% of the measured value. The experimental set-up is shown in fig. 6. The combined uncertainty of the experimental set-up is ±1.8% of the measured temperature. The DC power source, thermocouples, and the Pyranometer are connected to a data logger.

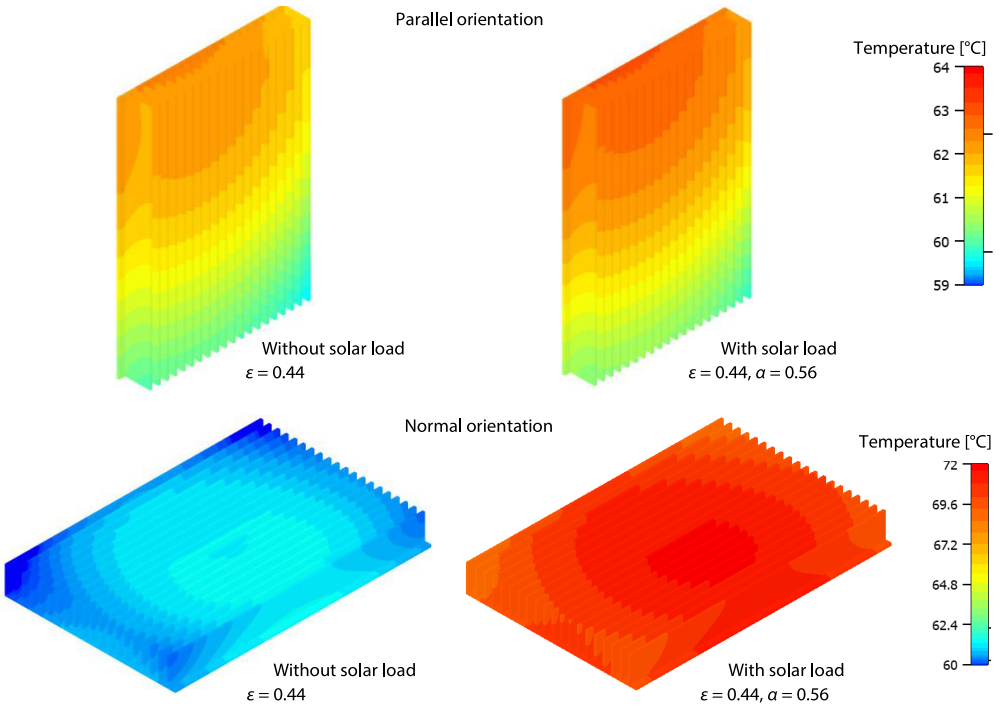

Figure 4. Temperature distribution on the heat sink for different orientations

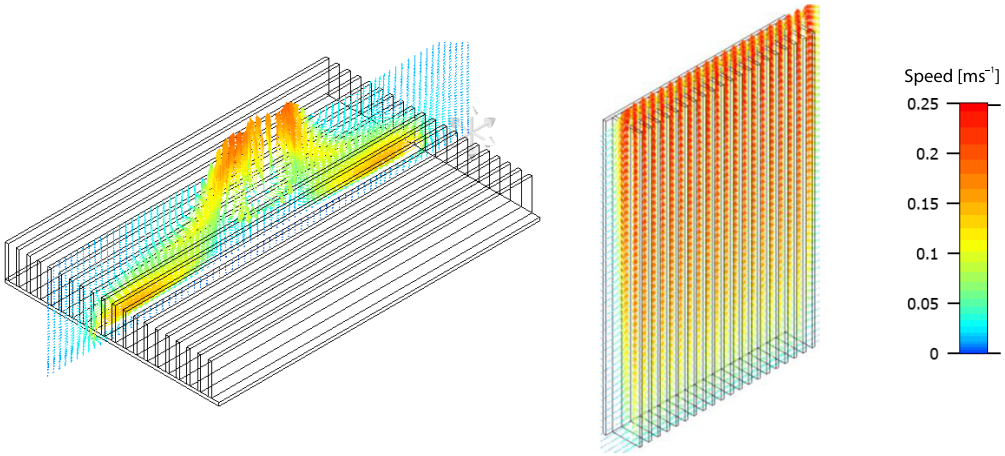

Figure 5. Velocity distribution on the heat sink for different orientations

The heat sink positioned in normal orientation gives a higher temperature thus the heat sink needs to be tested under normal orientation ensure the reliability of the electronic devices. The heat sink set-up is mounted on the terrace of the building to get it expose to solar radiation. The power resistor temperature, solar heat flux, and the power resistor supplied voltage are measured at a defined time interval and stored in the data logger. Temperature measurement is done at the center and four edges of the heat sink base using *T*-type thermocouples. Temperature is measured at a regular time interval until it reaches the steady-state condition. The center of the heat sink base exhibits the highest temperature and the same is reported here. The varia-

tion of temperature from the center to the edge is less than 1.0 °C. The measured solar flux is shown in fig. 7 and the measured heat sink base temperature is shown in fig. 8. The solar heat flux increases till 12:30 p. m. and decreases afterward. The solar heat flux varies from 395-857 W/m^2. The measurement is conducted for four consecutive days to ensure the repeatability of the experimental set-up. The solar heat flux trend concerning time repeats for all four days but the maximum solar irradiation varies from 857-882 W/m^2 from Day 1 to Day 4 due to weather changes.

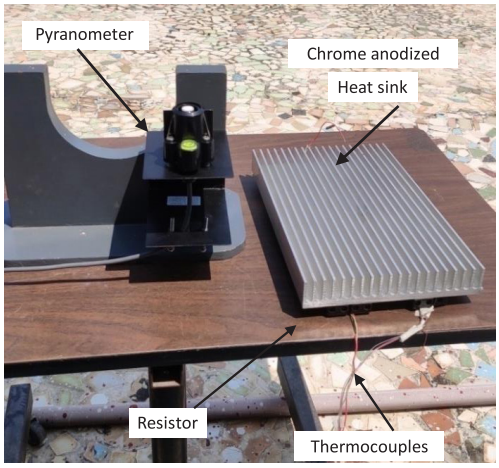

Figure 6. Experimental set-up for outdoor heat sink measurement

For Day 1 the heat sink base temperature increases up to 76.0 °C. The change in temperature over time follows the solar heat flux trend. To validate the simulation results with the measured results, the transient thermal simulation of the aforementioned said heat sink is conducted. A constant electronics heat load of 35 W and the variable solar heat flux measured on Day 1 are fed as input to the CFD tool. The emissivity of 0.44 and solar absorptivity of 0.56 are assumed on the heat sink surface to represent the chrome anodized finish. The transient thermal analysis is conducted and the heat sink temperature over time is predicted. The experimental and simulation results are shown in fig. 8. The maximum deviation in CFD results compared with the measured temperature is 3.8%.

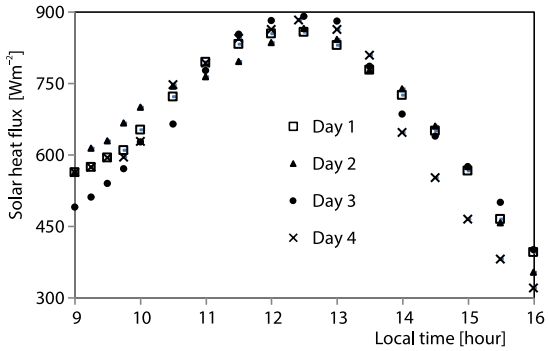

Figure 7. Measured solar heat flux

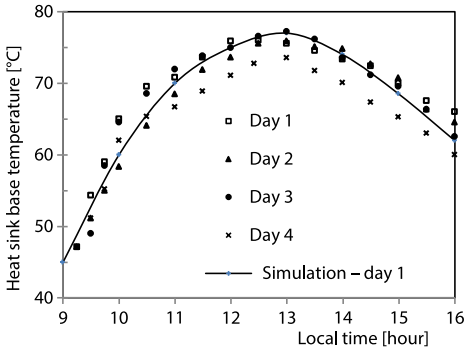

Figure 8. Comparison of measured heat sink base temperature with simulation results

Results and discussion

The temperature of the heat sink depends on heat sink orientation, fin height, and spacing between the fins. In addition the fin geometry, the surface finish also plays an important role in outdoor applications. It is proposed to conduct a parametric analysis to study the effect of solar irradiation and the radiation heat transfer. The length of the heat sink base is varied from 100-300 mm and the width of the base is varied from 100-300 mm. The fin height is varied from 10-30 mm. The 35 W of heat is applied at the base of the heat sink to represent the electronics devices and 600 W/m^2 of solar irradiation is also applied and the solar rays are normal to the ground.

Effect of solar absorptivity

The amount of solar heat absorbed by the heat sink surfaces depends on the orientation of the heat sink and the solar absorptivity. Table 1 shows the amount of solar heat absorbed by the heat sink for various configurations. In the parallel orientation, only the top edge of fins is exposed to the solar load, fig. 1. The solar heat absorbed in parallel orientation by the commercial finish heat sink with 100 mm width, 200 mm length, and 10 mm fin height, is only 0.14 W which is negligible compared to the electronics heat load. But the solar load absorbed by the same heat sink in normal orientation is 4.44 W which is 12.7% of the heat generated by the electronic devices. The solar heat absorbed by the black painted heat sink with the aforementioned said dimension is 0.37 W for parallel orientation and 11.56 W for normal orientation. Thus the solar heat absorbed by the black painted surfaces is 2.6 times more than the commercial finish heat sink and is 33% of the heat load generated by the electronics device. The solar heat absorbed by the various heat sink geometries for various surface finishes is given in tab. 1.

Table 1. Solar heat absorbed [W] by the heat sink surfaces for various configurations

Parallel orientation						
α	100 mm width			200 mm width		
	H 10 mm	H 20 mm	H 30 mm	H 10 mm	H 20 mm	H 30 mm
0.12	0.05	0.07	0.10	0.09	0.14	0.19
0.37	0.14	0.22	0.29	0.29	0.44	0.60
0.56	0.22	0.33	0.44	0.44	0.67	0.91
0.96	0.37	0.56	0.76	0.75	1.15	1.56
Normal orientation						
α	100 mm width			200 mm width		
	L 100 mm	L 200 mm	L 300 mm	L 100 mm	L 200 mm	L 300 mm
0.12	0.72	1.44	2.16	1.44	2.88	4.32
0.37	2.22	4.44	6.66	4.44	8.88	13.32
0.56	3.36	6.72	10.08	6.72	13.44	20.16
0.96	5.76	11.52	17.28	11.52	23.04	34.56

It is inferred that when the base area is increased to provide more fins to reduce the thermal resistance of the heat sink, the solar heat absorbed by the heat sink surface also increases considerably. For the case of 200 mm × 300 mm base area with black painted surfaces, the amount of solar heat load absorbed by the heat sink is 34.56 W almost equal to the heat generated by the electronics devices. In this case, the heat sink needs to be designed to dissipate 70 W of heat. The electronics heat load is 35 W which is only 50% of the total heat load on the heat sink and the remaining 50% is the solar heat absorbed by the fin surfaces. The area exposed to solar radiation in parallel orientation is almost 30 times less than that of normal configuration. The solar heat absorbed by the parallel orientation heat sink is 1.56 W which is almost 10 times lesser than that of normal orientation. More results are given in figs. 9 and 10. The change in heat sink length does not have any effect on the amount of absorbed solar heat for parallel orientation but the solar load increases when the width of the heat sink increases. For normal orientation both the change in width and length affect the amount of solar heat absorption.

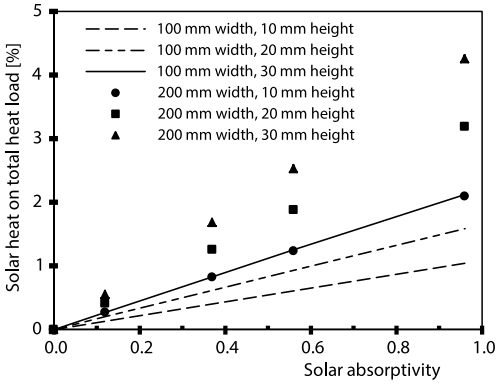

Figure 9. Contribution of solar heat on the total heat dissipation of the heat sink (parallel orientation)

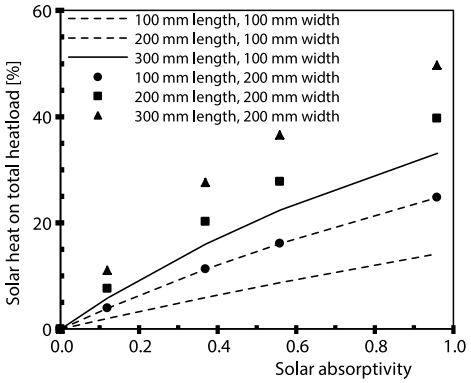

Figure 10. Contribution of solar heat on the total heat dissipation of the heat sink (normal orientation)

Effect of emissivity

The radiation heat transfer from the fin surfaces depends on the emissivity and is calculated using the simulationol. The amount of heat transferred by radiation from 100 mm × 100 mm commercial finish heat sink ($\varepsilon = 0.04$) is only 6.7% of the total heat load and the remaining heat is dissipated by convection. A similar heat sink with a black pained surface dissipates 46.8% of heat through radiation heat transfer. The convection heat transfer coefficient and the percentage of heat transferred by radiation for the normal configuration are shown in fig. 11. The average convective heat transfer coefficient of the fin decreases when the fin length increases, thus the convective heat transfer rate decreases. It is also understood that when the fin length increases the percentage of radiation heat transfer also increases. The percentage of heat transferred by radiation for various heat sink geometries is shown in fig. 12. The parallel and normal orientation of the heat sink exhibits the same behaviour since the orientation does not affect radiation heat transfer. The convection heat transfer rate changes due to the orientation effect and the percentage of radiation heat transfer in the normal configuration are 3% more than in the parallel configuration. When the fin height is increased from 5-30 mm heat sink base temperature

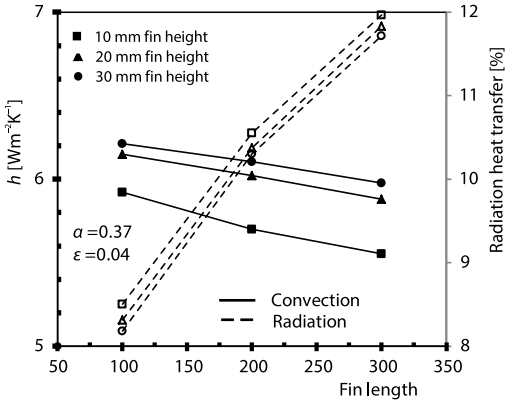

Figure 11. Combined convection and radiation heat transfer for normal configuration

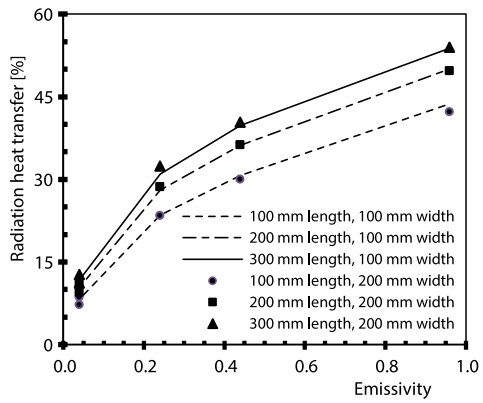

Figure 12. Percentage of radiation heat transfer

reduces from 64.7-51.9 °C. The base temperature reduces by 12.8 °C. When the emissivity is increased to 0.96 from 0.1 and the absorptivity is maintained as 0.1, heat sink base temperature reduces by 5.3 °C due to increased fin height. Similarly, for high absorptivity surfaces with $\alpha = 0.96$, the reduction in temperature due to increased fin height is 27.9 °C and 12.6 °C for low and high emissivity surfaces, respectively. The change in temperature due to fin height has a lesser effect on the high emissivity surfaces than the low emissivity surfaces. The effect on heat sink base temperature due to increased fin length is more for high absorptivity surfaces than low absorptivity surfaces.

Heat transfer and solar absorptivity

The normal orientation of the heat sink exhibits more solar heat absorption than the parallel orientation. Further, the analysis is conducted for normal orientation of the heat sink under solar irradiation predict the worst case temperature of the electronic device. The device temperature when it is attached to the commercial finish heat sink of base area 100 cm^2 and fin height 10 mm is 158.2 °C. The base temperature reduces to 138.6 °C for Al_2O_3 coated heat sink and 134.5 °C for Cr anodized heat sink. The device temperature further reduces to 123.2 °C for black painted surface ($\varepsilon/\alpha = 1.0$). As the heat sink base area increases the solar heat absorbed by the heat sink surface increases but the heat generated by the device remains constant. The heat sink temperature reduces due to the increased area available for convection and radiation. For the case of a commercial finish heat sink with 10 mm fin height the device temperature increases when the base area is increased beyond 700 cm^2. This is due to the solar heat absorbed by the fins increasing in proportion the base area but the average natural-convection heat transfer coefficient and the radiation heat transfer rate remain the same. For heat sink with 10 mm fin height the temperature increases beyond 700 cm^2 which is the optimum base area for all types of surface finishes as shown in fig. 13.

When the fin height is increased to 20 mm the optimum base area for black painted and Al_2O_3 coated heat sink can also be increased to 780 cm^2 and 850 cm^2, respectively, to reduce

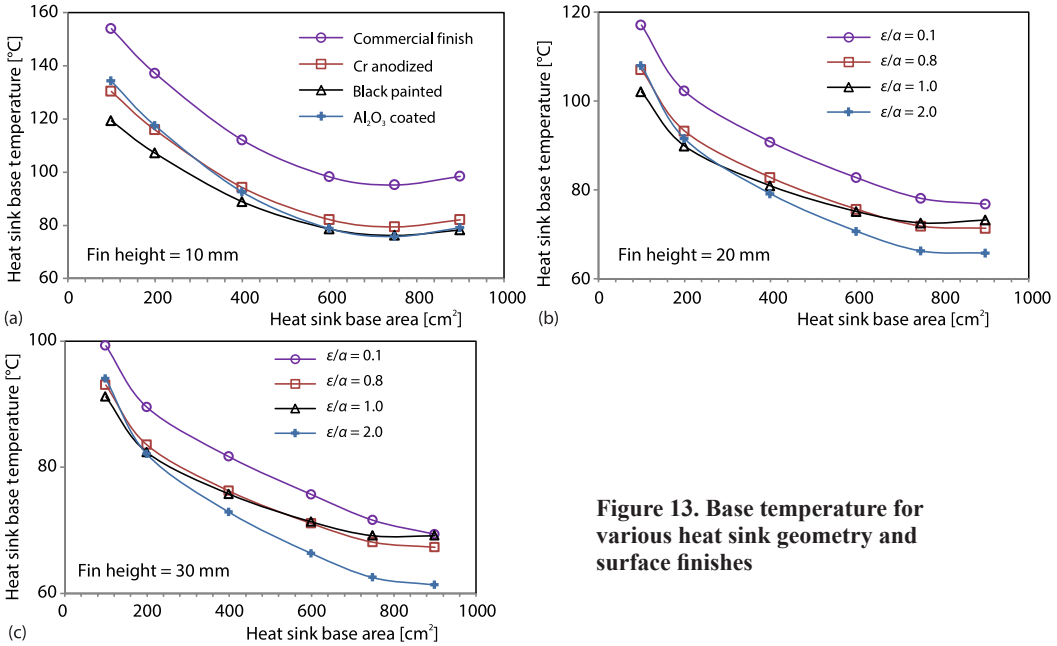

Figure 13. Base temperature for various heat sink geometry and surface finishes

the device temperature. When the fin height is increased to 30 mm the optimum base area can be increased to 900 cm^2 and the device temperature is brought down to 61.5 °C. The solar heat absorbed by the heat sink increases due to an increase in the base area but the increased fin height increases the heat transfer from the heat sink thus reducing the component temperature. The black painted surface exhibits the lowest temperature among the surface finishes, which is 15 °C less than that of the Al_2O_3 coated heat sink. The black painted surface is a good solar absorber as well as a good emitter of heat. As the heat sink base area increases the temperature difference between the Cr anodized and black painted heat sink reduces.

This is because though the Cr anodized and Al_2O_3 coated heat sinks are poor emitters compared to the black painted surface but the solar heat absorbed by these surfaces is also less. So the combined effect of solar absorptivity and emissivity improves the thermal performance of the Al_2O_3 coated and Cr anodized heat sinks at the higher base area. For the case of 20 mm and 30 mm fin height, the Al_2O_3 coated and Cr anodized heat sinks exhibit better performance than the black painted heat sink. When the fin height increases the convective heat transfer rate from the fin surfaces also increases for both black painted and Al_2O_3 coated surfaces. On the other hand, the view factor of the internal fin surface to the ambient decreases due to increased fin height. Thus the radiation heat transfer rate from the fin surfaces to the ambient decreases. It is understood that the radiation heat transfer is dominant in black painted heat sink and the same is affected by increased fin height. When the heat sink area increases the area exposed to solar irradiation also increases thus the solar heat absorbed by the heat sink increases. When the base area increases from 100 $mm^2 \times 100$ mm^2 to 200 $mm^2 \times 300$ mm^2, the convective heat transfer reduces from 6.2-6.0 W/m^2K. But the radiation heat transfer increases from 23-34%. Thus the combined heat transfer from the fin surfaces due to increased base area increases by 40%, and the base temperature reduction is more for higher base area. The heat sink base temperature decreases while increasing the heat sink base area, beyond a certain limit increase in base area of the heat sink produces an adverse effect due to increased solar heat absorption.

Conclusion

The contribution of radiation heat transfer and the effect of solar irradiation on the temperature of the electronic device due to different surface finishes are studied. It is found that the percentage of heat transfer by radiation varies from 6.2-11.0% for commercial finish surface and is as high as 58.7% for black painted heat sink surface. When the fin length increases the average heat transfer coefficient decreases thus the radiation heat transfer rate increases. The solar heat absorbed by the Al_2O_3 coated heat sink in normal configuration varies from 2.1-12.4% of the heat generated by the electronic devices. The Al_2O_3 coated and Cr anodized heat sinks exhibit better performance than the black painted heat sink at higher base area conditions.

Acknowledgment

This research work is supported by Society for Applied Microwave Electronics Engineering and Research, Ministry of Electronics and Information Technology, Govt of India.

Nomenclature

g – gravity force, [ms^{-2}]
H – fin height, [mm]
h – heat transfer co-efficient, [$Wm^{-2}K$]
k – thermal conductivity, [$Wm^{-1}K^{-1}$]
L – heat sink length, [mm]
q_v – internal energy, [W]
u, v, w – velocity in X-, Y-, and Z-direction, [ms^{-1}]
W – heat sink width, [mm]

Greek symbols

α – solar absorptivity
ε – emissivity
μ – viscosity, [$kgm^{-1}s^{-1}$]
ρ – fluid density, [kgm^{-3}]

References

[1] Agam, S., The 5G Unleashes the Future, *ASME Mechanical Engineering*, *141* (2019), 02, pp. 34-39
[2] Chen, Z., *et al*., Design and Simulation of the Thermal Management System for 5G Mobile Phones, in: *Advances in Heat Transfer and Thermal Engineering*, Springer, Singapore, Singapore, 2021
[3] Shang, Y., *et al*., The Design and Thermal Reliability Analysis of a High-Efficiency K-Band MMIC Medium-Power Amplifier with Multi harmonic Matching, in: *Active and Passive Electronic Components*, Hindawi Publishing Corporation, London, UK, Vol. 2016, p. 7
[4] Ellison, G. E., Maximum Thermal Spreading Resistance for Rectangular Sources and Plates with Non-Unity Aspect Ratios, *IEEE Transactions on Components and Packaging Technologies*, *26* (2003), 2, pp. 439-454
[5] Maguire, L., *et al*., Systematic Evaluation of Thermal Interface Materials – A Case Study in High Power Amplifier Design, *Microelectronics Reliability*, *45* (2005), 3-4, pp. 711-725
[6] Wang, X., *et al*., Effects of filler Distribution and Interface Thermal Resistance on the Thermal Conductivity of Composites Filling with Complex-Shaped Fillers, *International Journal of Thermal Science*s, *160* (2021), 106678
[7] Kraus, A. D., *et al*., *Extended Surface Heat Transfe*r, John Wiley and Sons Inc., New York, USA, 2001, Chapter 13, pp. 572-635
[8] Lee, S., Optimum Design and Selection of Heat Sinks, *Proccedings*, Eleventh IEEE SEMI-THERM Symposium, San Jose, Cal., USA, 1995, pp. 48-54
[9] Bar-Cohen, A., *et al*., Design of Optimum Plate-Fin Natural Convective Heat Sinks, *Journal of Electronic Packaging June*, *125* (2003), 2, pp. 208-216
[10] Liou, H. J., *et al.*, Revisit on the Natural-Convection from Horizontal Multi-Channel Rectangular-Fin Heat Sinks, *International Journal of Thermal Sciences*, *171* (2022), 107232
[11] Rao, R. V., Venkateshan, S. P., Experimental Study of Free Convection and Radiation in Horizontal Fin Arrays, *International Journal of Heat and Mass Transfer*, *39* (1996), 4, pp. 779-789
[12] Rao, D. V., *et al*., Heat transfer from a Horizontal Fin Array by Natural-Convection and Radiation – A onjugate Analysis, *International Journal of Heat and Mass Transfer*, *49* (2006), 19-20, pp. 3379-3391
[13] Wang, F. F., Electronics Packaging Simplified Radiation Heat Transfer Analysis Method, *Proceedings*, Inter Society Conference on Thermal Phenomena, Las Vegas, Nev., USA, 2004, pp. 613-617
[14] Yu, S. H., *et al*., Effect of radiation in a Radial Heat Sink under Natural-Convection, *International Journal o*f *Heat and Mass Transfer*, *55* (2012), 1-3, pp. 505-509
[15] Huang, L., *et al*., Cooling Strategy for LED Filament Bulb Utilizing Thermal Radiation Cooling and Open Slots Enhancing Thermal Convection, *Proceedings*, 16th IEEE ITHERM Conference, Orlando, Fla., USA, 2017, pp. 1030-1033
[16] Zhang, Z., *et al.*, The Role of Anodization in Naturally Cooled Heat Sinks for Power Electronic Devices, *ASME J. Heat Transfer*, *142* (2020), 5, 052901
[17] Zu, H., *et al.*, Analysis of enhanced Heat Transfer on A Passive Heat Sink with High-Emissivity Coating, *International Journal of Thermal Sciences*, *166* (2021), 106971
[18] Ganesan, D., Ramalingam, V., Effect of Solar Irradiation on Thermal Performance of Heat Sink – Numerical and Experimental Study, *IEEE Transactions on Components, Packaging and Manufacturing Technology*, *11* (2021), 9
[19] ***, IEEE Std C37.24™-2017, IEEE Guide for Evaluating the Effect of Solar Radiation on Outdoor Metal-Enclosed Switchgear, 2017
[20] Churchill, S. W., Chu, H. H. S., Correlating Equations for Laminar and Turbulent Free Convection from a Vertical Plate, *International Journal of Heat and Mass Transfer*, *18* (1975), 11, pp. 1323-1329
[21] Mubarak, R., *et al*., Improving the Irradiance Data Measured by Silicon-Based Sensors, *Energies*, *14* (2021), 2766

Paper submitted: January 10, 2023
Paper revised: February 24, 2023
Paper accepted: March 7, 2023